General Disclaimer

One or more of the Following Statements may affect this Document

- This document has been reproduced from the best copy furnished by the organizational source. It is being released in the interest of making available as much information as possible.

- This document may contain data, which exceeds the sheet parameters. It was furnished in this condition by the organizational source and is the best copy available.

- This document may contain tone-on-tone or color graphs, charts and/or pictures, which have been reproduced in black and white.

- This document is paginated as submitted by the original source.

- Portions of this document are not fully legible due to the historical nature of some of the material. However, it is the best reproduction available from the original submission.

NT

NASA
Technical Memorandum 81732

AVRADCOM
Technical Report 81-C-6

A Sputtered Zirconia Primer for Improved Thermal Shock Resistance

R. C. Bill
Propulsion Laboratory
AVRADCOM Research and Technology Laboratories
Lewis Research Center
Cleveland, Ohio

and

J. Sovey and G. P. Allen
Lewis Research Center
Cleveland, Ohio

Prepared for the
Third International Conference on Wear of Materials
San Francisco, California, March 30-April 1, 1981

NASA

A SPUTTERED ZIRCONIA PRIMER FOR IMPROVED THERMAL SHOCK RESISTANCE OF PLASMA-SPRAYED CERAMIC TURBINE SEALS

by R. C. Bill
Propulsion Laboratory
AVRADCOM Research and Technology Laboratories
Lewis Research Center
Cleveland, Ohio

and

J. Sovey and G. P. Allen
National Aeronautics and Space Administration
Lewis Research Center
Cleveland, Ohio

SUMMARY

Considerable process has been achieved in the development of plasma-sprayed yttria stabilized zirconia (YSZ) ceramic turbine blade tip seal components. The YSZ layers are quite thick (0.040 to 0.090 in.) compared to typical thermal barrier coating layers applied to airfoils, which are more effectively cooled than the seal. The service potential of seal components with such thick ceramic layers are cyclic thermal shock limited. The most usual failure mode is ceramic layer delamination at or very near the interface between the plasma-sprayed YSZ layer and the NiCrAlY bondcoat. Deposition of a thin RF sputtered YSZ primer to the bondcoat prior to deposition of the thick plasma-sprayed YSZ layer has been found to reduce laminar cracking in cyclic thermal shock testing. The cyclic thermal shock life of one ceramic seal design was increased by a factor of 5 to 6 when the sputtered YSZ primer was incorporated. A model based on thermal response of plasma-sprayed YSZ particles impinging on the bondcoat surface with and without the sputtered YSZ primer provides a basis for understanding the function of the primer.

E-742

INTRODUCTION

In commercial aviation, fuel costs now account for more than one-half of the direct operating costs of the aircraft fleet (ref. 1). Therefore, any method of improving engine efficiency will have a significant impact on transportation cost. A very effective way of improving gas turbine engine efficiency is to reduce clearances over the tips of the turbine blades shown schematically in figure 1. Approximately 1 percent improvement in engine efficiency can be realized for each 1 percent reduction in the ratio of tip clearance to blade span (ref. 2).

In order to maintain reduced tip clearances and achieve the full potential of improved turbine tip seal technology, the turbine shroud material must be: (1) abradable, that is, be easily worn in the event of a rub interaction with the blade tips; (2) erosion resistant; (3) oxidation and corrosion resistant; and (4) able to withstand the thermal shock environment imposed by engine operation. Currently used metallic turbine tip seal materials tend to cause blade tip wear through adhesive material transfer. Furthermore, they require substantial amounts of cooling air to prevent erosive and oxidative material loss. Recent results have shown that turbine shroud systems employing plasma-sprayed yttria stabilized zirconium oxide (YSZ) adjacent to the gas path show considerable promise from the standpoints of potentially higher operating temperatures (less cooling air) and improved abradability (refs. 3 and 4). The challenge, however, is to make these systems so that they are thermal shock resistant. Because of heat flux considerations and allowing for abradability, the ceramic layers employed in turbine shroud applications are four to five times as thick as typical thermal barrier coatings. Hence, some especially severe thermal shock-related problems arise (ref. 5).

There are basically two methods of reducing thermal stresses imposed on the plasma-sprayed YSZ turbine shroud system as the engine goes through its spectrum of transient and steady-state conditions. One method is to grade the composition of the system from fully metallic adjacent to the metal substrate to fully ceramic adjacent to the gas path. The graded composition can be optimized so that thermal stresses are controlled to an acceptable level throughout a specified thermal cycle (ref. 6). Another approach, with perhaps more flexibility, is to provide a strain isolator layer between the ceramic layer and the metal substrate. The strain isolator layer concepts that have shown promise include sintered porous fibermetal materials and thick, plasma-sprayed porous metal layers (refs. 7 and 8).

Experimental results have shown that thermal shock failures, when they occur, tend to originate at the interface between the fully ceramic layer and the intermediate layer. Hence, improvement in thermal shock resistance is expected if the bond between the YSZ layer and the substrate system (first graded layer, or strain isolator layer) can be improved. Various methods of doing this were evaluated, and one method incorporating a sputtered YSZ "primer" applied directly to the substrate system prior to deposition of the plasma-sprayed YSZ appeared promising.

In this paper, plasma-sprayed YSZ turbine shroud systems incorporating two different strain isolator materials serve as baseline. The objectives are to (1) compare the cyclic thermal shock resistance of the baseline specimens with that of specimens incorporating a sputtered YSZ primer coat and (2) identify the mechanisms of interaction between the sputtered YSZ primer and the plasma-sprayed YSZ layer.

APPARATUS AND PROCEDURE

The cyclic thermal shock apparatus is shown in figure 2(a). An oxygen-acetylene torch provides the means of heating the specimen when it is in the "heat-up" position, with the flame impinging directly onto the ceramic surface at a 90° angle. While the ceramic surface is being heated, cooling air is directed onto the specimen backing. The flame is positioned and tuned so that during the heat-up phase the ceramic surface reaches a stable temperature of about 1315° C within 1 minute for all seal configurations. Total duration of the "heat-up" phase is 3 1/2 minutes. Cooling air flow to the

backing is controlled to 2.4×10^{-3} m^3/sec (5 ft^3/min) for all specimens, with associated backing temperatures of 480° to 540° C, depending on specimen configuration. Ceramic surface temperatures are monitored by an infrared pyrometer, and were cross-checked by chromel alumel thermocouples embedded in a few special calibration specimens. Accuracy of the pyrometer measurements is believed to be within 50° C of the actual surface temperature. Temperatures at other locations in the seal and on the metallic backing are measured by chromel-alumel thermocouples in all specimens.

After being held in the flame for 3 1/2 minutes, the specimen is moved by means of the pneumatic actuator into the "cool-down" position. During the cool-down phase, which lasts for 1 minute, a cooling air flow of 1.2×10^{-3} m^3/sec (2.5 ft^3/min) is directed onto the ceramic surface in addition to the 2.42×10^{-3} m^3/sec (5 ft^3/min) flowing over the back surface. The ceramic surface was thereby cooled from its maximum of 1315° to about 450° C in several seconds. By the end of the cool-down phase the entire specimen is at about 300° C. The cycle is then repeated. A simplified time-temperature schedule representative of the entire thermal cycle is shown in figure 2(b). Temperatures are indicated for the ceramic surface and the metallic backing. Not indicated in figure 2(b) is a 10-15 second time delay between the start of cooldown on the ceramic surface and the first indication of cooldown on the backing.

MATERIALS

The specimens evaluated in this study incorporated either one of two different types of strain isolator layers between the dense metal substrate and the plasma-sprayed ceramic layer. In all cases the substrate was a 50 mm x 25 mm x 9 mm thick 304 stainless steel block. The overall specimen configuration is shown in figure 3(a).

One type of strain isolator layer material employed consisted of a 3-mm thick pad of sintered, low-density, Fe-25 w/o Ni-18 w/o Cr-9 w/o Al-0.02 w/o Y (FeNiCrAlY) fibermetal brazed directly to the substrate. Density of the fibermetal was 32 percent (i.e., 68 percent open porosity), and the fiber diameter was 35 μm. Figure 3(b) shows a representative microstructure of this material.

The second type of strain isolator layer consisted of porous plasma-sprayed Ni-16 w/o Cr-6 w/o Al-0.6 w/o Y (NiCrAlY) deposited to a 1.75-mm thickness. The desired porosity level of approximately 50 percent was obtained by co-spraying the NiCrAlY with polyester, then baking out the polyester after specimen fabrication. The bakeout temperature of 500° C is not believed to be high enough to promote any significant stress relief in the sprayed porous layer. The microstructure of this material is shown in figure 3(c).

Following application of the strain isolator layer to the 304 stainless steel substrate, a 50-μm thick NiCrAlY bondcoat was plasma-spray deposited onto the strain isolator layer. Specimens that were to incorporate the sputtered YSZ primer were then taken to the sputter facility while the control specimens without the primer were withheld until all specimens (primer and control) were ready for plasma-sprayed YSZ application.

Sputter deposition of zirconia was performed using a 10-cm diameter argon ion beam source with a plasma bridge neutralizer. The zirconia sputter target (30 cm diameter) was located 15 cm from the ion source at an angle of 45 degrees with respect to the beam. The substrate was parallel to the target and separated from the target by 15 cm.

Deposition procedures are as follows:

(1) Ion clean the sputter target for 2.5 hours at an ion energy of 1200 eV and an ion current density of 0.5 mA/cm^2. Pressure was 5×10^{-5} torr.

(2) Outgas the substrate at 5×10^{-7} torr for 45 minutes.

(3) Ion clean the target for 5 minutes.

(4) Ion clean the substrate for 5 minutes at 1200 eV, 0.5 mA/cm^2.

(5) Adjust an air leak into the vacuum chamber until the pressure reaches 1×10^{-3} torr. Sputter deposit zirconia at 1300 eV and 0.5 mA/cm^2 for 18 1/2 hours to yield a zirconia film thickness of about 1.5 μm.

The as-sputtered deposited YSZ film on a plasma-sprayed NiCrAlY substrate is shown in figure 4.

The YSZ powder employed for plasma-spraying was ZrO_2 - 12 w/o Y_2O_3, and the particle size was -200 + 325 mesh. Using the Plasmadyne SG-1 plasma spray gun, the following parameters were employed: 550 ampere arc current, 4.6×10^{-4} m^3/sec arc gas (Argon) flow rate, 9.3×10^{-5} m^3/sec powder gas flow rate, with the powder feed setting at 3.0. The plasma-sprayed YSZ coating was deposited to a thickness of about 2.1 mm. The plasma-sprayed materials and parameters are essentially those developed by Liebert and Stecura (ref. 9) for thermal barrier application.

RESULTS

General

The experimental results are summarized in figure 5. Incorporation of the sputtered YSZ primer in specimens with the sprayed porous NiCrAlY intermediate layer resulted in a five- to six-fold improvement in cyclic thermal shock life. This improvement is substantially more than three standard deviations above the baseline life for specimens without the sputtered YSZ primer.

Specimens incorporating the sintered FeNiCrAlY intermediate layer, both with and without the sputtered YSZ primer, consistently survived 1000 cycles. One thousand cycles was selected as run-out for purposes of the ceramic seal thermal shock test program.

By way of putting the above results into perspective, YSZ layers applied to a 2.1-mm thickness without any intermediate layer system (a standard NiCrAlY bondcoat was used) consistently and completely spalled early in the heat-up transient of the first cycle (ref. 7). Further discussion of the experimental results will be divided into two sections, one pertaining strictly to specimens with the sprayed porous NiCrAlY intermediate layers, and the other to specimens with the sintered FeNiCrAlY intermediate layer.

Sprayed Porous NiCrAlY

Specimens prepared in the manner described in the Materials section, both with and without the primer, failed in essentially the same manner. A substantial portion of the sprayed YSZ layer (25 to 75 percent) underwent delamination at or near the interface with the NiCrAlY bondcoat, as shown in figures 6(a) and (b). However, it appears that more plasma-sprayed YSZ is retained on the failure surface of the specimens with the sputtered YSZ primer than without. This implies an improvement in bond strength with use of the primer, and is consistent with substantially longer lives of specimens incorporating the primer.

Note that in figure 5, results include data from specimens in which the 2.1-mm plasma-sprayed YSZ layer was deposited under conditions of increased standoff distance and reduced plasma-spray intensity. These altered spray conditions result in a more porous and compliant plasma-sprayed YSZ layer, with a consequent reduction in stresses induced by the thermal cycle (ref. 7). An interesting difference between the failure mode of these specimens and those prepared using standard spray parameters for the YSZ deposition is observed. Figure 6(c) shows failure as occurring primarily within the YSZ layer for the case of the reduced density YSZ. Little or no bondcoat is actually exposed on the failure surface. Apparently the bondcoat/YSZ interface is not the weak link in these specimens. For reduced density YSZ specimens with and without the sputtered YSZ primer, a similar number of cycles is required to initiate cracks within the YSZ and propagate those cracks to failure.

Sintered FeNiCrAlY

Metallographic sections were prepared in order to examine the integrity of the interface between the plasma-sprayed YSZ layer and the bondcoat after 1000 cycles of thermal shock testing. Figure 7 reveals a significant difference, depending on whether or not a sputtered YSZ primer was used. In figure 7(a), for the specimen with the primer, only isolated discontinuous laminar cracking was observed. Furthermore, there appeared to be no interaction between cracks propagating through the sprayed YSZ layer down to the bondcoat region and the occurrence of laminar cracking.

In contrast, after 1000 cycles, extensive laminar cracking (somewhat exaggereated by particle pull-out during metallographic preparation) had occurred over most of the YSZ/bondcoat interface of specimens without the primer, as may be seen in figure 7(b). Also, the laminar cracks and cracks propagating through the ceramic layer are observed to have joined. The particular specimen shown in figure 7(b) was probably not very far from failure.

DISCUSSION

The reasons for improved bonding of the plasma-sprayed YSZ layer to the substrate when the sputtered YSZ primer was used are not clearly understood. One explanation is that the sputtered YSZ coating covers the NiCrAlY bondcoat more continuously than does the first layer of plasma-sprayed YSZ. Plasma-sprayed YSZ in turn wets the sputtered YSZ more readily than it would wet the NiCrAlY bondcoat, thereby giving a stronger interfacial bond. The sputtered surface itself, shown in figure 4, provides a very fine scale surface roughness of its own, superimposed on the bondcoat roughness, possibly enhancing the available bond area.

An additional effect, potentially promoting improved bonding, may be attributed to the thermal insulative properties of the sputtered YSZ primer relative to the bondcoat. Consider the initial cooling and solidification rate of the first layer of plasma-sprayed YSZ particles as they impinge on the bondcoat surface with and without the sputtered primer. The situation is shown schematically in figure 8. In order to examine the significance of the presence of the primer, it is assumed that the initial temperature of the impinging molten YSZ particles is approximately the "melting temperature," T_m (3035 K for pure ZrO_2). Assume also that the bondcoat and primer initial temperature T_o is approximately 478 K, typical of available data from spray operations without substrate temperature control. At time t,

after impingement, the location of the liquid/solid interface ℓ in the solidifying plasma-sprayed particle is given by

$$\ell = at^{1/2} \tag{1}$$

where a is

$$a = \frac{2[T_m - T_o]\exp\left(\frac{-a^2}{4\alpha_c}\right)}{H\sqrt{\frac{\pi\rho_c}{C_c K_c}}\left[\sqrt{\frac{\rho_c C_c K_c}{\rho_s C_s K_s}} + \operatorname{erf}\frac{a}{2\sqrt{\alpha_c}}\right]} \tag{2}$$

according to reference 10. In equation (2), subscript c refers to the impinging ceramic particle, whereas subscript s denotes properties for the substrate, either the NiCrAlY bondcoat or the sputtered YSZ primer. Equation (2) was solved for a with and without the primer, and the location of the solidification front as it moves through the particle is plotted in figure 9 for both cases. Also shown in figure 9 is the location of the second solidification front driven by radiation cooling from the exposed surface of the particle. The particle is assumed to be 25 μm thick. The results summarized in figure 9 bear two important points pertaining to particle bonding: (1) The time of solidifcation is significantly increased if the primer is present, possibly resulting in a more compact and cohesive first layer of plasma-sprayed ceramic particles as described by Helgesson (ref. 11). (2) Since the final solidifcation in the particle occurs nearer the particle centroid when the primer is present, residual stresses tending to lift the particle edges would be reduced.

The calculations performed above, of course, are based on many assumptions that are not strictly accurate on the time and dimensional scale of interest. Certainly the bondcoat or primer is rapidly heated to a depth that is not really negligible compared to particle thicknesses. Also, ZrO_2 -12%Y_2O_3 does not have a discrete melting temperature, but rather a melting range. Nevertheless, with these reservations about quantitative accurracy in mind, the calculations are believed to show a real and significant solidification rate effect.

SUMMARY OF RESULTS

Cyclic thermal shock experiments were conducted on specimens simulating two different turbine seal candidate systems. The systems differed in the type of strain isolator intermediate layer employed between the plasma-sprayed YSZ layer and the substrate. The effect of the presence of a sputter deposited YSZ layer applied to the NiCrAlY bondcoat prior to deposition of the plasma-sprayed YSZ layer was assessed. The following conclusions were drawn from these experiments:

(1) Application of the sputtered YSZ primer resulted in a five- to six-fold improvement in thermal shock life of specimens with a sprayed porous NiCrAlY intermediate layer.

(2) Specimens with and without the primer survived 1000 cycles (run-out) when a sintered FeNiCrAlY intermediate layer was used. Significantly

reduced laminar cracking was observed in the specimen with the primer however.

(3) The improvements attributed to the sputtered YSZ primer are believed to be due to two contributions. First, the plasma-sprayed YSZ particles more effectively wet and adhere to the bondcoat when the YSZ primer is present than when it is not. Second, the cooling and solification rate of impinging, molten plasma-sprayed YSZ particles is retarded when the primer is present, allowing for the formation of a more compact first layer of sprayed particles with a less detrimental residual stress distribution.

SYMBOLS

a	solidification rate coefficient, $m/sec^{1/2}$
C_C	specific heat of ZrO_2, 0.13 cal/(gm)(K)
C_S	specific heat of substrate, 0.1 cal/(gm)(K) for NiCrAlY
H	heat of fusion of ZrO_2, 20.8 K cal/gm mole
K_C	thermal conductivity of ZrO_2, 1.57 W/(m)(K)
K_S	thermal conductivity of substrate, 15.7 W/(m)(K)
	instantaneous position of solidifcation front, m
T_m	melting temperature of ZrO_2, 3035 K
T_O	substrate temperature, 478 K
α_a	thermal diffisivity of ZrO_2, 0.21×10^{-2} m^2/hr
ρ_C	density of ZrO_2, 5.6 gm/cm^3
ρ_S	density of substrate, 8 gm/cm^3 for NiCrAlY

REFERENCES

1. L. P. Ludwig, NASA TM 73890, 1978.
2. R. J. Roelke, Miscellaneous Losses, in Turbine Design and Applications, Vol. 2, A. J. Glassman, ed., NASA SP-290, 1973, p. 125.
3. R. C. Bill, L. T. Shiembob, and O. L. Stewart, NASA TM-79022, 1978.
4. D. L. Clingman, B. Schechter, K. R. Cross, and J. R. Cavanaugh, NASA CR-159739, 1979.
5. F. E. Kennedy and R. C. Bill NASA TP-1437, 1979.
6. L. T. Shiembob, NASA CR-135183, 1977.
7. R. C. Bill, D. W. Wisander, and D. E. Brewe, NASA TP-1561, 1980.
8. A. F. Erickson, J. C. Nablo, and C. Panzera, ASME Paper 78-WA/GT-16, Dec. 1978.
9. S. Stecura and C. H. Liebert, Thermal Barrier Coating System. U.S. Patent No. 4,055,705, Oct. 1977.
10. W. M. Rohsenow and J. P. Hartnett, eds., Handbook of Heat Transfer. McGraw Hill, N. Y., p. 3.
11. C. I. Helgesson, Transactions of the Xth International Ceramics Congress, C. Brosset and C. Helgesson, eds., Stockholm, Sweden, 1966, p. 393.

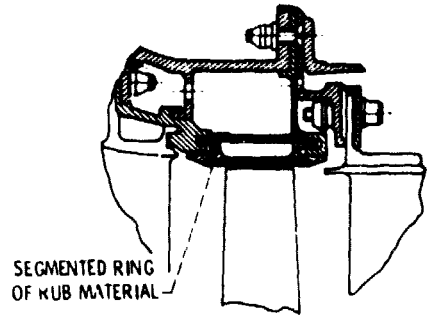

Figure L. - Schematic of high-pressure-turbine outer air seal.

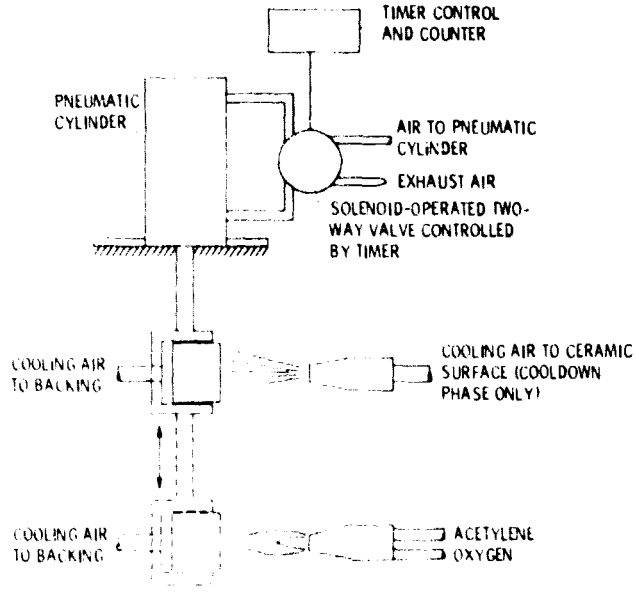

(a) THERMAL SHOCK APPARATUS.

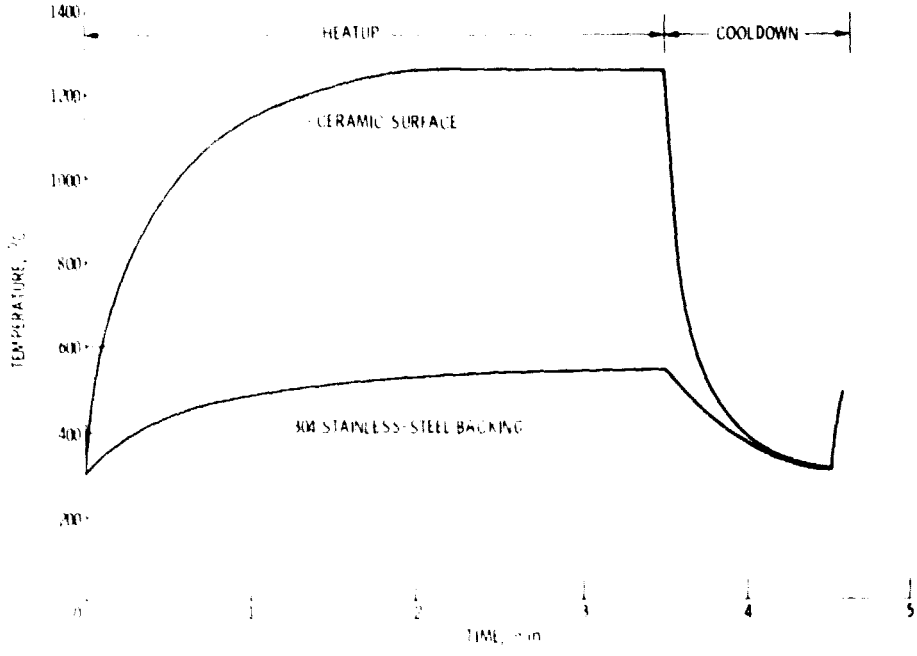

(b) REPRESENTATIVE TIME-TEMPERATURE PLOT FOR THERMAL SHOCK CYCLE.

Figure 2. - Thermal shock rig and test cycle

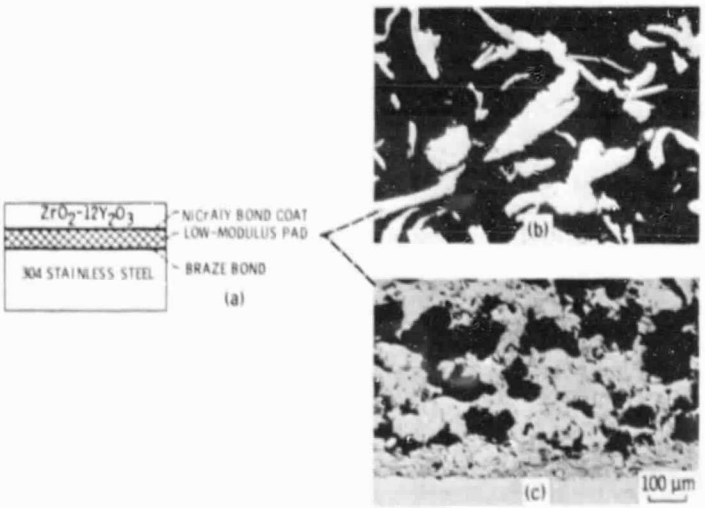

Figure 3. - (a) Overall specimen configuration.
(b) Plasma-sprayed porous NiCrAlY strain isolater layer.
(c) Sintered porous FeNiCrAlY strain isolator layer.

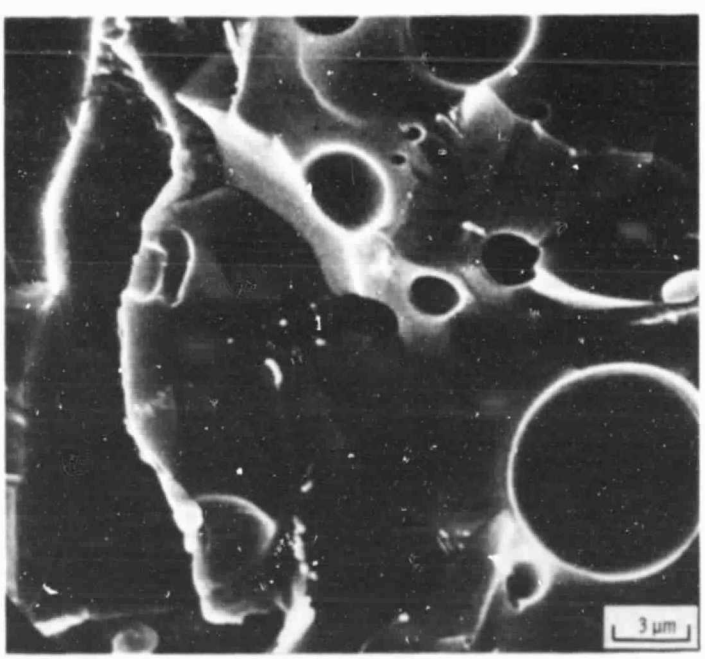

Figure 4. - Sputter deposited YSZ on plasma-sprayed NiCrAlY bondcoat surface.

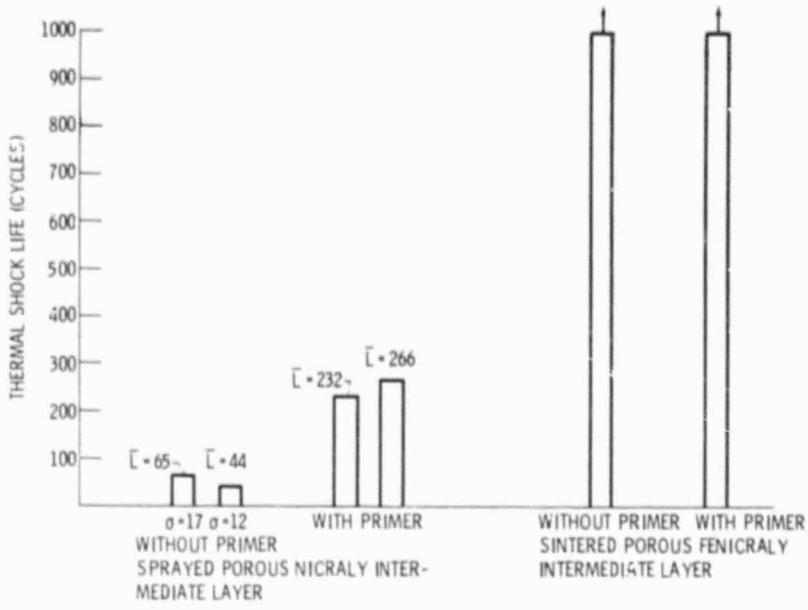

Figure 5. - Results of cyclic thermal shock experiments.

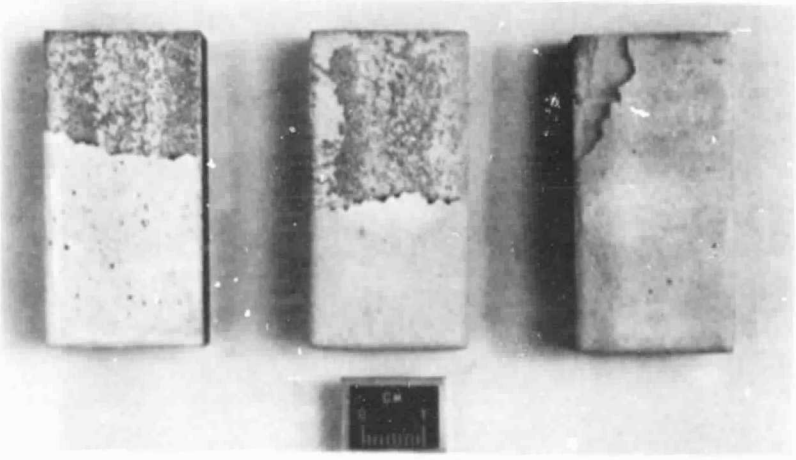

(a) BASELINE (WITHOUT PRIMER).

(b) WITH SPUTTERED YSZ PRIMER.

(c) WITH LOW DENSITY PLASMA-SPRAYED YSZ LAYER.

Figure 6. - Thermal shock specimens after failure.

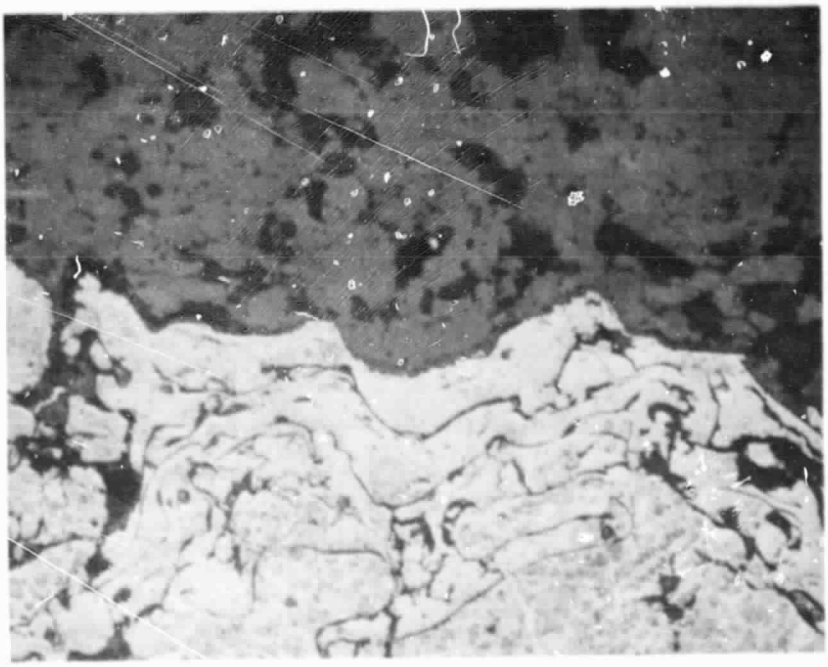

(a) WITH SPUTTERED YSZ PRIMER.

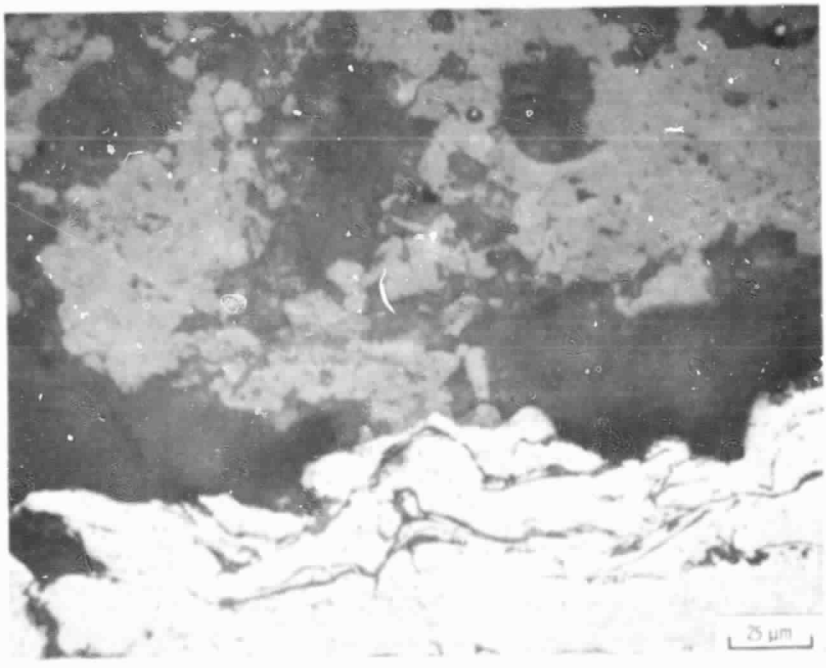

(b) WITHOUT PRIMER.

Figure 7. - Microsections through YSZ/bondcoat interface after 1000 thermal shock cycles.

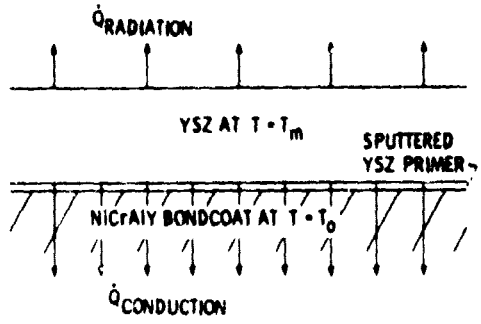

Figure 8. - Molted plasma-sprayed YSZ particle solidification, schematic.

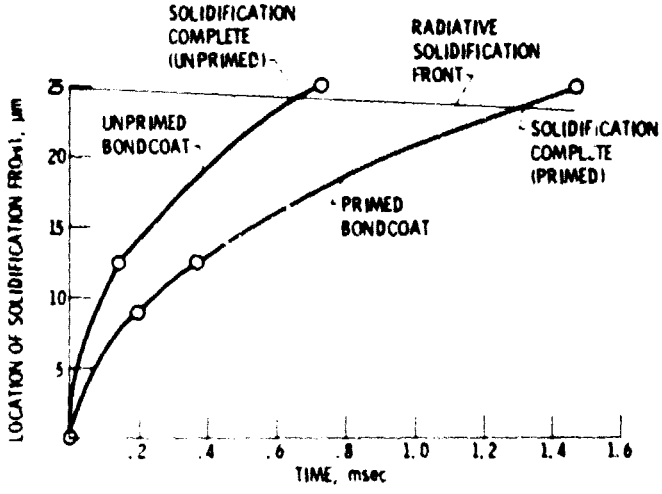

Figure 9. - Progression of solidification through molten plasma-sprayed YSZ particle after impingement upon sputter deposited YSZ primed NiCrAlY bondcoat, and unprimed NiCrAlY bondcoat.